Available online at www.sciencedirect.com

ScienceDirect

Biomedical Journal

journal homepage: www.elsevier.com/locate/bj

Original Article

# Nrf2 activation attenuates the early suppression of mitochondrial respiration due to the α-synuclein overexpression

Mu-Hui Fu [a], Chih-Wei Wu [b], Yu-Chi Lee [b], Chun-Ying Hung [b], I-Chun Chen [b], Kay L.H. Wu [b,c,*]

[a] Department of Neurology, Kaohsiung Chang Gung Memorial Hospital, Kaohsiung, Taiwan
[b] Institute for Translational Research in Biomedicine, Kaohsiung Chang Gung Memorial Hospital, Kaohsiung, Taiwan
[c] Department of Senior Citizen Services, National Tainan Institute of Nursing, Tainan, Taiwan

ARTICLE INFO

*Article history:*
Received 12 December 2017
Accepted 13 February 2018
Available online 6 July 2018

*Keywords:*
A53T
α-synuclein
ROS
Mitochondrial respiration
Mitochondrial biogenesis
Nrf2

ABSTRACT

*Background:* α-synuclein (SNCA) accumulation in the substantia nigra is one of the characteristic pathologies of Parkinson's disease (PD). A53T missense mutations in the SNCA gene has been proved to enhance the expression of SNCA and accelerate the onset of PD. Mitochondrial dysfunction in SNCA aggregation has been under debate for decades but the causal relationship remains uncertain. At a later stage of PD, the cellular dysfunctions are complicated and multiple factors are tangled. Our aim here is to investigate the mitochondrial functional changes and clarify the main causal mechanism at earlier-stage of PD.
*Methods:* We used the mutant A53T SNCA-expressed neuro 2a (N2a) cells without detectable cell death to investigate: 1) whether SNCA overexpression impairs the mitochondrial respiration and biogenesis. 2) The role of nuclear factor (erythroid-derived 2)-like 2 (Nrf2) signal in SNCA–induced mitochondria dysfunction.
*Results:* Accompanying with the increment of SNCA, reactive oxygen species (ROS) accumulation was increased. The maximal respiratory capacity was suppressed. Meanwhile, mitochondrial complex 1 activity and the activity of nicotinamide adenine dinucleotide (NADH) cytochrome C reductase (NCCR) were decreased. Moreover, the mitochondrial DNA (mtDNA) copy number was decreased. On the other hand, the nuclear peroxisome proliferator-activated receptor-gamma coactivator 1α (PGC-1α), Nrf2, and the cytosolic mitochondrial transcription factor A (TFAM) were increased at an early stage and declined thereafter. Above factors triggered by SNCA were reversed by tBHQ, a Nrf2 activator.
*Conclusion:* These results suggested that at an early stage, SNCA-overexpressed increase mtROS accumulation, mitochondrial dysfunction and mtDNA decrement. Nrf2, PGC-1α and TFAM were upregulated to compromise mitochondrial dysfunction. tBHQ effectively reversed the SNCA-induced mitochondrial dysfunction.

* *Corresponding author*. Institute for Translational Research in Biomedicine, Kaohsiung Chang Gung Memorial Hospital, 123, Dabi Rd., Niausung, Kaohsiung 833, Taiwan.
E-mail address: klhwu@cgmh.org.tw (K.L.H. Wu).
Peer review under responsibility of Chang Gung University.
https://doi.org/10.1016/j.bj.2018.02.005

## At a glance of commentary

### *Scientific background on the subject*

Parkinson disease (PD) is a chronic irreversible neurodegenerative disease. Ala53Thr missense point mutation of a-synuclein gene (SNCA) induces a faster SNCA aggregation and more severe motor disability via reactive oxygen species (ROS) accumulation and mitochondrial dysfunction. However, why PD onset long after a period of well motor function is unclear.

### *What this study adds to the field*

Our study demonstrates that Nrf2, the hub of endogenous antioxidant and mitochondrial biogenesis, upregulates to against the ROS accumulation and renew mitochondria during early SNCA accumulation. Nrf2 exhausted with accumulating mitochondrial ROS contribute to dampened mitochondrial biogenesis and the sequel PD pathological switch on.

Lewy body (LB) is the most pivotal pathological hallmark of Parkinson's disease (PD), and mainly distributes in the neuronal cell body and neurites of substantia nigra [1,2]. The main composition of LB is α-synuclein (SNCA). SNCA is a small 140-amino-acid protein mainly found in presynaptic terminals of neurons [3]. Previous studies indicated that approximately 90% of SNCA deposited in LB is phosphorylated at serine 129 (pS129), while only 5% of pS129 SNCA is detected in normal brains [4–7]. SNCA phosphorylation and aggregation are accelerated by missense point mutations of SNCA gene (*SNCA*), including Ala30Pro (A30P), Ala53Thr (A53T) and Glu46Lys (E46K) [8–10]. Studies from SNCA transgenic mice indicate that A53T mutant induces a faster SNCA aggregation [11] and more severe motor disability [6,12–14] than A30P mutant strain. E46K has been documented not only able to aggregate SNCA [15,16], but enhance SNCA phosphorylation [17] even faster than the previously discovered two mutations [18]. Though only 10% of PD patients are familial cases [19], the pathological picture of SNCA aggregation is identical to most sporadic cases. Therefore, knowing how SNCA overexpression dampens neuronal functions becomes a critical issue.

Neuron is highly demanding for energy support to maintain its function, including synaptic plasticity. Mitochondrial aerobic respiration is the major pathway to generate ATP. Oxygen consumption rate (OCR) is a fundamental index of mitochondrial aerobic respiration. Maximal respiratory capacity from OCR represented an indicator of energetic reserve capacity to meet a sudden demand of energy, particularly in high-energy requiring tissues [20]. Electron transport chain reaction (ETC) is a key element of ATP production. The electron transportation from mitochondrial respiratory complex 1 (Mt cpx1, known as NADH dehydrogenase) or Mt cpx2 (succinate dehydrogenase) to Mt cpx3 by electron carrier (coenzyme $Q_{10}$, Q) is the common pathway to generate the driving forces of ATP production. SNCA accumulation has been demonstrated to cause mitochondrial dysfunction [21,22] and inhibits Mt cpx1 [23]. Damage of Mt cpx1 by oxidant results in mitochondrial dysfunction and causes PD [24]. These reports suggest the interaction of SNCA and mitochondrial function under the development of PD.

ROS-induced mtROS generation has been proposed in other studies [25]. Overexpression of SNCA is a primary initiator of reactive oxygen species (ROS) at basal status in neural cells [26]. Mitochondrial ROS (mtROS) is a side product of electron transportation mainly from Mt cpx1 to Mt cpx3. Impairment of Mt cpx1 enhances the production of mtROS, which may trigger the sequel mitochondrial damages. It is likely that SNCA-induced ROS impairs Mt cpx1 for the mtROS generation. Nuclear factor (erythroid-derived 2)-like 2 (Nrf2) is an inducible transcription factor which encodes many antioxidant proteins, including heme oxygenase-1 (HO-1), ubiquitin/PKC-interacting protein A170, peroxiredoxin 1, the heavy and light chains of ferritin, catalase, glutathione peroxidase, superoxide dismutase, and thioredoxin [27]. According to previous studies, Nrf2 deficiency aggravates SNCA-associated protein aggregation [28]. On the other hand, overexpression of Nrf2 ameliorates neurodegeneration in Drosophila model of PD [29]. However, why Nrf2 does not properly diminish the ROS and renew mitochondria in the SNCA-overexpressed neurons is largely unknown.

Mitochondrial biogenesis plays an important role in controlling mitochondrial quality by generating new mitochondria to replace the damaged parts. In response to the request of new and healthy mitochondria, the peroxisome proliferator-activated receptor γ coactivator 1-α (PGC-1α) translocate to nucleus and interact with transcription factors, such as Nrf2, for encoding mitochondrial transcription factor A (TFAM) to transcript and translate mitochondrial DNA (mtDNA) [30]. SNCA overexpression has been reported to damage mtDNA [31]. Although there is no sufficient evidence to link SNCA overexpression and the dysregulation of mitochondrial biogenesis, it is conceivable that SNCA overexpression may trigger sustained mtROS accumulation, damage mtDNA, and eventually destroy the quality control of mitochondria.

Several mechanisms involved in the pathogenesis of PD including mitochondrial dysfunction [32]. Though mitochondrial dysfunction has been linked to PD most frequently, the results from different studies varied widely because of dynamical interaction between the intracellular signaling pathways and different microenvironment. The pathogenic features of mitochondria can be more complex during the course of SNCA accumulation far before cell death. In the present study, we used the *in vitro* model of human A53T mutant SNCA in the dopaminergic cell line, N2a cells. To avoid the observation at later and irreversible stage, we conducted a low-toxic level of SNCA up-regulation with no apparent cell death which was defined as an earlier-stage of SNCA accumulation. The interplay of SNCA overexpression and mitochondrial dysfunction was evaluated under an early-PD simulating condition.

## Materials and methods

### *DNA construction*

The human SNCA was constructed from A53T, which was generated through designing PCR primer with point mutation

G to A in the 157th nucleotide. To detect the gene expression more easily, flag tag was inserted to the 3' end of SNCA. The whole construct was driven by a human ubiquitin promoter (Fig. 1A). FUGW is a lentiviral vector that carries the human ubiquitin promoter driving a GFP reporter gene (Fig. 1B) and being used as a negative control in our experiment.

### Cell culture and transfection

N2a mouse neuroblastoma (N2a; ATCC) cells were maintained in Eagle's minimum essential medium (MEM; Invitrogen), 1 mM sodiumpyruvate (Sigma) and 10% (v/v) heat-inactivated fetal bovine serum (Hyclone), 100 U/mL penicillin, and 100 μg/mL streptomycin (Invitrogen). Cells were incubated in a humidified incubator at 37 °C in 5% $CO_2$. One day before transfection, cells were plated in growth medium without antibiotics. The content of transfection mixture included DNA, Opti-MEM® I Reduced Serum Medium without serum, and Lipofectamine™ 2000. After dripping the mixture into cells, the cells were incubated at 37 °C in a $CO_2$ incubator for 48-hrs prior test.

### MTS assays for cell viability

3-(4,5-dimethylthiazol-2-yl)-5-(3-carboxymethoxyphenyl)-2-(4-sulfophenyl)-2H-tetrazolium (MTS) assay (Promega, Madison, WI, USA) was used to quantify cell viability following the guideline of the kit. In brief, N2a cells (100 μL, $1 \times 10^5$ cells/ml) were seeded into a 96-well flat-bottomed plate for 24 hrs at 37 °C with 5% $CO_2$ then subjected to plasmid transfection. At 24 h after transfection, the cells were washed with PBS and replaced with 100 μL fresh medium. Followed, the cells were further treated with vehicle or antioxidants for 24 hrs. After washed by PBS, 20 μL MTS reagents were added to each well, and the plate was incubated for 4 hrs under dark. Absorbance was recorded at 490 nm using a microplate reader (Thermo Fisher Scientific Inc.). Blank wells with no reagent were measured for luminescence and were deducted from the values of the experimental wells. Values of viability of the treated-cells were expressed as a percentage of that from corresponding control cells. All experiments were repeated in triplicates.

### CellTiter-Glo® 2.0 assay for cell proliferation

CellTiter-Glo® 2.0 Assay (Promega) was used to evaluate the cell proliferation following the guideline of the kit. In brief, $1 \times 10^4$ N2a cells were seeded into a 96-well flat-bottomed plate for 24 h at 37 °C with 5% $CO_2$ then subjected to plasmid transfection. At 24 hrs after transfection, the cells were washed with PBS and replaced with 100 μL fresh medium. Followed, the cells were further treated with vehicle or antioxidants for 24 hrs. After washed by PBS, 100 μL of CellTiter-Glo® 2.0 Reagent were added to each well, and the plate was incubated for 12 min on an orbital shaker for cell lysis at room temperature. The Luminescence was recorded. Blank wells with no reagent were measured for luminescence and were deducted from the values of the experimental wells. Values of proliferation of the treated-cells were expressed as a percentage of that from corresponding control cells. All experiments were repeated in triplicates.

### Cell Death Detection ELISA$^{PLUS}$ for cell death

Cell Death Detection ELISA$^{PLUS}$ (Roche) was used to evaluate the cell death following the guideline of the kit. In brief, $1 \times 10^4$ N2a cells were seeded into a 96-well flat-bottomed plate for 24 hrs at 37 °C with 5% $CO_2$ then subjected to plasmid transfection. At 24 hrs after transfection, the cells were washed with PBS and replaced with 100 μL fresh medium. Followed, the cells were further treated with vehicle or antioxidants for 24 hrs. After washed by PBS, 200 μL of lysis buffer were added to each well, and the plate was incubated for 30 min on an orbital shaker for cell lysis at room temperature. The lysate was centrifuged at 200 $\times g$ for 10 min to obtain the supernatant. 20 μL of the supernatant was incubated with 20 μL Immunoreagent for 2 hrs. After washed by Incubation buffer, 100 μL of ABTS solution was added to each well for 20 min. After 100 μL of Stop solution was added to each well, the luminescence was detected at 405 nm. Blank wells with no reagent were measured for luminescence and were deducted from the values of the experimental wells. Apoptosis of the treated-cells were expressed as a percentage of that from corresponding FUGW transfected cells. All experiments were repeated in triplicates.

### Mitochondrial respiratory rate detection by the XF analyzer

XF24 Extracellular Flux Analyzer were used to perform all XF assays (Seahorse Bioscience; MA, USA). The sensor cartridge contains four reagent delivery chambers per well for injecting compounds, including inhibitors of mitochondrial respiratory complex I (rotenone), III (antinomycin A), IV (FCCP) and V (oligomycin), into the wells during an assay to evaluate the rates of oxygen ($O_2$) consumption rate (OCR) and changes in extracellular acidification rates (ECAR). For cellular detection, $1 \times 10^5$ N2a cell were seeded into XF24 plates for overnight attachment (except for background correction wells). After various time intervals of treatments, culture medium was washed out by PBS and substituted by 1X MAS buffer (Seahorse Bioscience) with substrate. The plate was then transferred to the XF24 instrument to initiate the measurement.

### Nuclear and cytosolic protein extraction

In some of the experiments, nuclear and cytosolic proteins were extracted by protocol described previously [33]. Collected cells samples from each group were homogenized with a Dounce grinder with a loose pestle in iced-chilled CelLytic™ MT Cell Lysis Reagent (Sigma–Aldrich) with a protease inhibitor cocktail (Sigma–Aldrich) to prevent protein degradation. The homogenate was centrifuged at 2000 x $g$, 4 °C, 10 min, 4 °C and the supernatant was collected as cytosolic fraction. After washed with ice-cold PBS, the pellet was resuspended in lysis buffer (10 mM HEPES, pH 7.2, 15 mM $MgCl_2$, 10 mM KCl, 1 mM PMSF, 2 mM NaF, 15 μg/ml leupeptin, and 1 mM sodium orthovanadate) on ice for 10 min and followed by samples lysing with a tight pestle. The homogenate was then centrifuged at 4000 $g$, 4 °C, 10 min. To rupture the nuclear membrane, the pelleted nuclei were resuspended in 15–20 μl of extraction buffer

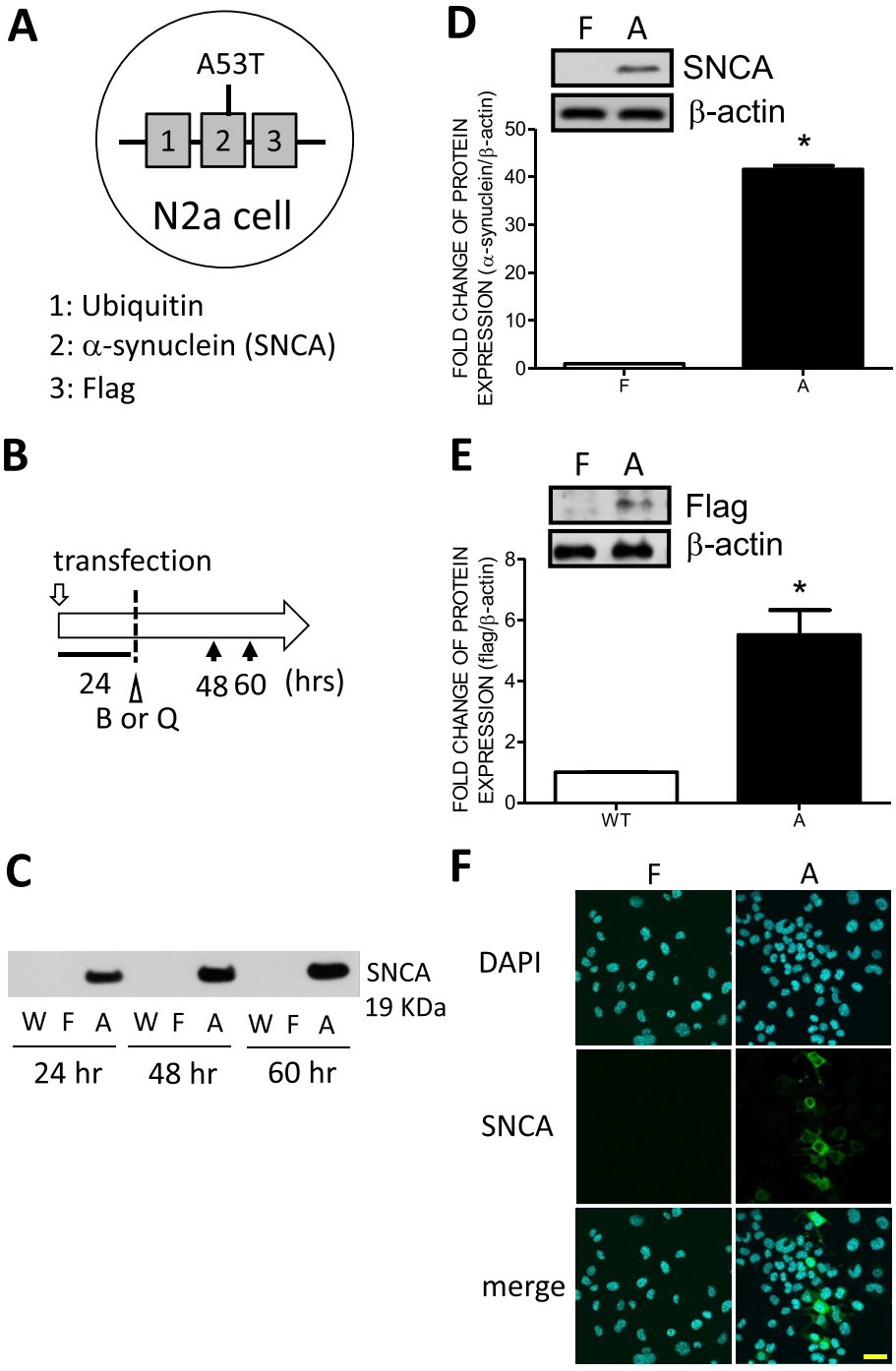


Fig. 1 **Increased expression of α-synuclein in N2a cells by human α-synuclein A53T mutant transfection.** (A) The construct of mutant α-synuclein (SNCA) contained A53T by point mutated G→A in the 157th nucleotide. Flag was fused with mutant SNCA and the whole construct was driven by a human ubiquitin promoter. The FUGW control was construct by the human ubiquitin promoter inserted into the lentiviral vector. (B) The scheme of experiment procedures. (C) 24-, 48- and 60-hr after transfection, the expression of SNCA showed a time-dependent increment in A53T N2a cells and was undetectable in W or F groups. Representative gels and densitometric analyses of SNCA (D) and Flag (E) 48 h of F and A groups. (F) Immunofluorescence images of nuclei (DAPI, blue) and SNCA (green) 48 h of FUGW or A53T groups. A: A53T mutant transfected N2a cells; WT: naïve N2a cell; F: N2a cell transfected with FUGW. β-actin as loading control. Values are mean ± SEM, n = 4 in each experimental group. *$p < 0.05$ versus F group in the Student *t* tests. Abbreviations used: B: tert-Butylhydroquinone, tBHQ, a Nrf2 activator; Q: coenzyme $Q_{10}$. Scale bar: 20 μm.

(100 mM HEPES, pH 7.2, 1.5 mM MgCl2, 1 mM EDTA, 0.8% NaCl, 15% glycerol, 2 mM NaF, 1 mM PMSF, 15 μg/ml leupeptin, and 1 mM sodium orthovanadate) and incubated on ice for 2–4 h. The nuclear suspension was centrifuged at 14,000 x *g*, 4 °C, 30 min, and the supernatant was saved as nuclear protein for further analyses. The purity of protein from the nuclear-rich and cytosolic fractions were verified by the expression of TATA-binding protein (TBP) and glyceraldehyde 3-phosphate dehydrogenase (GAPDH) protein, respectively. Protein concentration was determined by Micro BCA Protein Assay kit (Thermo Fisher Scientific Inc.).

### *Assays for activity of mitochondrial respiratory enzymes*

Activities of electron transport of the mitochondrial respiratory chain were performed immediately after mitochondrial isolation, using a thermostatically regulated ThermoSpectronic spectrophotometer (Thermo Fisher Scientific, Hertfordshire, UK) [34].

To determinate the activity of nicotinamide adenine dinucleotide (NADH) cytochrome C reductase (NCCR; the electron transport from Complexes I to III), the mitochondrial fraction (20 μg of protein) was incubated in a mixture containing 50 mM $K_2HPO_4$ buffer, pH 7.4, 1.5 mM KCN, 1 mM β-NADH at 37 °C for 2 min. After the addition of 100 μM cytochrome *c*, the reduction rate of oxidized cytochrome *c* was measured at 550 nm for 3 min at 37 °C. The molar extinction coefficient of cytochrome *c* at 550 nm is 18,500 M/cm.

For the activity of succinate cytochrome C reductase (SCCR; the electron transport from Complexes II to III), the mitochondrial fraction (30 μg) was performed in 40 mM $K_2HPO_4$ buffer (pH 7.4), 1.5 mM KCN, supplemented with 20 mM succinate. After a 5-min equilibration at 37 °C, 50 μM cytochrome *c* was added and the reaction was monitored at 550 nm for 3 min at 37 °C.

At least duplicate determination was carried out for each sample in these enzyme activity assays, and the activity was expressed as nmol/μg protein/min. All reagents used in enzyme assays will be purchased from Sigma–Aldrich.

### *Total protein isolation*

Collected cells samples from each group were homogenized with a Dounce grinder with a tight pestle in ice-cold lysis buffer (15 mM HEPES, pH 7.2, 60 mM KCl, 10 mM NaCl, 15 mM $MgCl_2$, 250 mM sucrose, 1 mM EGTA, 5 mM EDTA, 1 mM PMSF, 2 mM NaF, 4 mM $Na_3VO_4$). A mixture of leupeptin (8 μg/mL), aprotinin (10 μg/mL), phenylmethylsulfonyl fluoride (20 μg/mL) and trypsin inhibitor (10 μg/mL) was included in the isolation buffer to prevent protein degradation. The homogenate was centrifuged at 13,500 *g* for 10 min at 4 °C, and the supernatant was collected for protein analysis. The concentration of the total protein extracted was estimated by the method of Bradford with a protein assay kit (Bio-Rad, Hercules, CA).

### *Western blotting*

After transfection, cells were rinsed with cold PBS and harvested using 100 μL lysis buffer (20 mM Tris-base, 150 mM NaCl, 1 mM ethylenediaminetetraacetic acid, 1 mM ethylene glycol tetraacetic acid, 1% Triton X-100, 2.5 mM sodium pyrophosphate, 1 mM β-glycerophosphate, 1 mM $Na_3VO_4$). The lysate was centrifuged (12,000 × *g*, 12 min, 4 °C) and the supernatant was stored at −80 °C for later use. Protein concentration was determined using a Micro BCA protein assay kit (Thermo Fisher Scientific; Waltham, MA). Total proteins were separated by sodium dodecyl sulfate (SDS) polyacrylamide gel electrophoresis, using 8, 10 or 12.5% gels and a running buffer of 24 mM Tris–HCl, 0.19 M glycine, 0.5% SDS, pH 8.3. Proteins were transferred to polyvinylidene difluoride (PVDF) membranes in transfer buffer (20 mM Tris–HCl, 150 mM glycine, 10% methanol, 0.05% SDS). The membranes were incubated in blocking buffer (Tris-buffered saline containing 5% nonfat dry milk and 0.1% Tween-20) at room temperature for 1 h. After washing, the membranes were incubated with primary antibodies overnight at 4 °C. Immunoblots were probed with primary antibodies, including anti-α- synuclein (1:10,000; BD Bioscience, San Jose, CA, USA), M2-flag (1:1000; Sigma–Aldrich, St. Louis, MO, USA), anti-Nrf2 (1:1000, Biovision, Milpitas, CA, USA), anti-p-Nrf2 (1:1000, Biorbyt Ltd., Cambridge, United Kingdom), anti-peroxisome proliferator-activated receptor-γ coactivator 1 α (PGC-1α, 1:1000; Thermo Fisher Scientific, Waltham, MA, USA), anti- Mitochondrial transcription factor A (TFAM, 1:1000; Thermo Fisher Scientific) antibodies were used. β-actin, prohibitin and TATA binding protein (TBP) served as the internal control of cytosolic, mitochondrial and nuclear fractions, respectively.

### *Immunofluorescence staining*

To evaluate the efficiency of A53T mutant α-synuclein transfection, the N2a cells were firstly rinsed with PBS and fixed by methanol. The cells were subjected to incubate with anti-α-synuclein (1:750, BD Bioscience, San Jose, CA, USA) at 4 °C overnight and then rinsed 3 times in PBS. After incubation in Alex 488 conjugated anti-rabbit or mouse IgG (1:500; Invitrogen) for 2 hrs, the cells were rinsed 3 times in PBS for further observation.

To evaluate the accumulation of reactive oxygen species (ROS) in mitochondria of the N2a cells, MitoSOX staining was applied in red fluorescence. Firstly, the living cells were rinsed with PBS and were subjected to incubate with MitoSOX (5 μM, Invitrogen™, CA, USA) for 15 min at 25 °C. Then, the cells were rinsed with PBS 3 times to wash out free form MitoSOX. The images of cells with increased mitochondrial ROS accumulation were analyzed by a confocal microscope (FluoView FV10i, Olympus).

The distribution of SNCA, total Nrf2, p-Nrf2, PGC-1α and TFAM in N2a cells were detected by the immunoreaction with antisera of Nrf2 (1:1000, Abcam, Cambridge, MA, USA), p-Nrf2 (1:1000, Abcam), PGC-1α (1:1000, Abcam), SNCA (1:1000, Abcam) and anti-NeuN (1:1000, Millipore, Darmstadt, Germany), a neuronal marker. In brief, the cells were incubated at 4 °C overnight and then rinsed 3 times in PBS. After incubation in Alex 488 or Alexa 594 conjugated anti-rabbit or mouse IgG (1:500; Jackson Invitrogen) for 2 h, the cells were rinsed 3 times in PBS. Cells were then observed under a confocal microscope (FluoView FV10i, Olympus).

### Genomic DNA extraction

To isolate genomic DNA, QIAamp DNA Mini Kit (QIAGEN, Hilden, Germany) was used according to the manufacturer's protocol. In brief, the harvested $5 \times 10^6$ N2a cells were incubated at 56 °C for 10 min with 200 μL buffer AL with proteinase K. Then, incubated with RNase A for 2 min at room temperature. Followed, 200 μL Buffer AL per sample was added and incubated at 70 °C for 10 min 200 μL 100% ethanol was gentle mixed to the sample and was applied to the QIAamp Mini spin column for centrifugation at 6000 x *g* for 1 min. The column was then washed by 500 μL Buffer AW1 and centrifuged at 6000 x *g* for 1 min 500 μL Buffer AW2 was then applied for a serial centrifugation that is 20,000 x *g* for 3 min followed by another centrifugation at 20,000 *g* for 1 min. The column was incubated with 20–30 μL water at 65 °C for 5 min, and then centrifuged at 6000 *g* for 1 min to elute the genomic DNA.

### Mitochondrial DNA copy number detection

To identify the differences of mtDNA copy number between groups, the ratio of cDNA amplified from mtDNA-encoded NADH dehydrogenase subunit 1 (ND1) to nucleus-encoded 18S rRNA genes were evaluated as previous described [35]. In brief, primers for the ND1 probe corresponded to nucleotides 389–408 (forward) and 572–592 (reverse; PCR product of 200 base pairs) of the rat mitochondrial genome (Chromosome MT–NC_001665.2). The primer sequences used for mtDNA copy number detection were: ND1 (mtDNA encoded NADH dehydrogenase-1), Forward (5′-3′) TCGGAGCCCTACGAGCCGTT/Reverse (5′-3′) AGGGAGCTCGATTTGTTTCTG. 18S rRNA served as controls for mtDNA for reaction efficiency. Primers for the 18S probe corresponded to nucleotides 681–702 (forward) and 864–884 (reverse; PCR product of 200 base pairs) of the rat nuclear genome (Chromosome 14–NC_005113.3). The primer sequences were: Forward (5′-3′) TAGTTGGATCTTGGGAGCGGG/Reverse (5′-3′) CCGCGGTCCTATTCCATTATT. The quantitative real-time polymerase chain reaction (qPCR) was performed in a Roche LightCycler 480 (Roche Applied Science, Mannheim, Germany) apparatus with the LightCycler 480 SYBR Green I Master kit (Roche Molecular Systems, Inc., Basel, Swiss). The DNA (50 ng) was mixed with 10 μL LightCycler 480 SYBR Green I Master Mix that contained 5 μmol (final concentration 0.4 μM) of forward and reverse primers in a final volume of 10 μL. The qPCR reactions were conducted as follows: denaturation at 95 °C for 10 min, 40 cycles of amplification at 95 °C for 10 s, annealing at 60 °C for 20 s, and extension at 72 °C for 10 s. Melting at 95 °C for 5 s, 65 °C for 60 s, then immediately raised to 97 °C followed by cooling to 40 °C for 30 s. The value was determined for each individual qPCR run. The $\Delta Ct = [Ct (ND1) - Ct (18S)]$ represents the relative abundance. The quantitative results were expressed as the copy number of mtDNA/sample by $2^{-\Delta Ct}$. Each measurement was at least triplicate and normalized in each experiment against serial dilutions of a control DNA sample.

### Statistical analysis

Data are expressed as means ± SEM. The data were analyzed by unpaired student's t-test and one-way ANOVA. The statistical significance was determined by the one-way ANOVA followed by the Bonferroni multiple comparison test. The differences were considered statistically significant when $p < 0.05$. Calculations were performed by GraphPad Prism (version 5) software (GraphPad Software, San Diego, CA).

## Results

### A53T mutant enhanced the expression of SNCA in N2a cell without induced cell death

Accumulation of SNCA and mitochondrial dysfunction in neurons are major pathological hallmarks in PD. However, the causal relationship between SNCA accumulation and mitochondrial dysfunction is still inconclusive. To avoid observation at later and irreversible stage, we conducted a low-toxic level of SNCA up-regulation to dissect the interplay of SNCA and mitochondrial function. A53T mutant plasmids were transfected to increase the expression of SNCA in dopaminergic cell line, N2a cells. To evaluate the efficiency of SNCA transfection by lentiviral backbone plasmid (FUGW), we detected the protein expression of SNCA in N2a cells transfected with FUGW or A53T mutant at 24-, 48-, and 60-hrs after transfection (Fig. 1B). SNCA was undetectable in wild type (W) and FUGW (F) but was significantly upregulated in A53T mutant-transfected cells (A) in a time-dependent manner. According to the Western blot analyses, the expression of SNCA was significantly increased in a dose dependent manner and up to 40-folds at 48-hrs in comparison with FUGW group and was plateaued at 60-hrs (Fig. 1C). Therefore, post-transfected 48-hrs was selected to further delineate the interaction of mitochondrial functions and SNCA accumulation. The expression of SNCA was detected by Western blot analyses to demonstrate the upregulation after A53T transfection. In comparison with FUGW transfected N2a cells, the level of SNCA in A group was significantly increased (Fig. 1D). To ensure the source of SNCA upregulation, we detected the flag signal to confirm the increment of SNCA in A53T transfected cells (Fig. 1E). The efficiency of transfection was further evaluated by immunofluorescence. The N2a cells with the expression of SNCA in cytosol appeared in green fluorescence while rare SNCA was detected in FUGW transfected cells (Fig. 1F). The cell viability, cell proliferation and apoptosis assays further indicated that no significant differences between F and A groups at 48 hrs post-transfection (Suppl. 1A, 1B and 1C).

### tBHQ reversed the A53T induced reactive oxygen species (ROS) accumulation in the mitochondria of N2a cells

Reactive oxygen species (ROS) are highly reactive molecules to oxidize protein, DNA and lipids, but oxidative stress is generated as a byproduct. Oxidative stress has been highlighted as the possible underlying mechanism of PD in genetic mouse models [36]. Mitochondria are major sources of ROS generation. To delineate whether SNCA increased the level of mitochondrial ROS (mtROS), cells from each group were stained with MitoSOX (red fluorescence; an index of

mitochondrial ROS) and MitoTracker (green fluorescence; an index of mitochondrial mass) and being detected by confocal microscopy. In this study, mtROS was prominently accumulated in A53T cell (Fig. 2). The images indicated that increased SNCA expression boosted mtROS accumulation, in accompany with mitochondrial mass decrement. Both tert-Butylhydroquinone (tBHQ) and coenzyme $Q_{10}$ are well known antioxidants for ROS scavenge while tBHQ is a Nrf2 activator and Coenzyme $Q_{10}$ serves as an electron carrier in mitochondrial ETC. On the other hand, less mtROS were detected in FUGW and tBHQ (10 μM)-treated groups (AB) with higher content of mitochondrial mass. Coenzyme $Q_{10}$-treatment (AQ, 1 μM) showed no effect on eliminating mtROS.

### *tBHQ reversed the A53T mutant transfection induced the nuclear factor erythroid 2-related factor 2 (Nrf2) expression in N2a cells*

The nuclear factor erythroid 2-related factor 2 (Nrf2) regulates mitochondrial biogenesis [35], and capable of accelerating the clearance of SNCA accumulation [37]. According to the Western blot analyses, the total expression of nuclear Nrf2 protein in A53T mutant N2a cell was significantly enhanced when compared with FUGW cells (Fig. 3A). Immunofluorescent images further indicated that the nuclear Nrf2 was decrease in AB and AQ groups (Fig. 3B).

On the other hand, the expression of nuclear p-Nrf2 (Fig. 3C) showed no significantly changes when compared

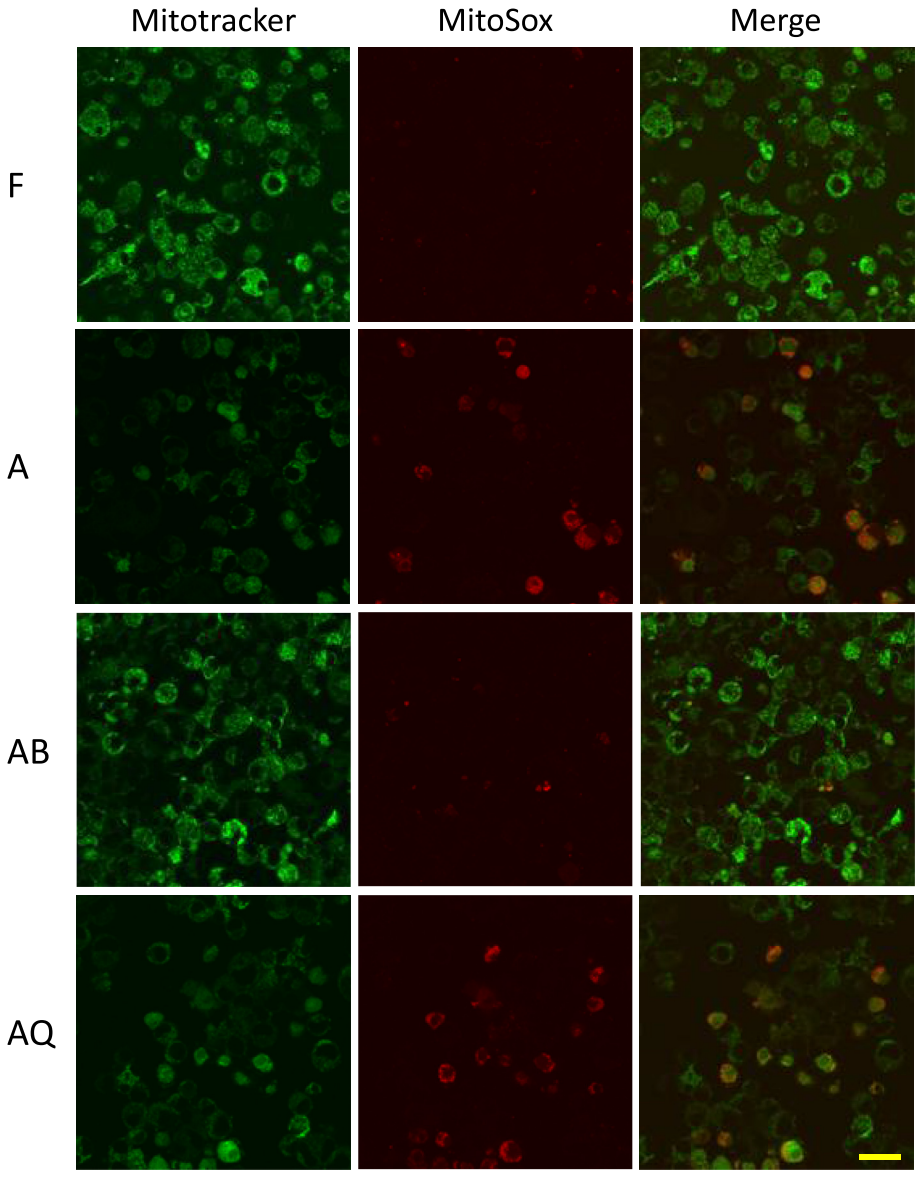


Fig. 2 **The increase of mitochondrial ROS in A53T mutant transfected N2a cells was reduced by tBHQ.** Immunofluorescence images of MitoTraker (an index of mitochondrial mass, green) and MitoSOX (an index of mitochondrial ROS, red) staining at 48 h of F, A, AB and AQ groups. Abbreviations used: A: A53T mutant transfected N2a cells; F: N2a cell transfected with FUGW; B: tert-Butylhydroquinone, tBHQ, a Nrf2 activator; Q: coenzyme $Q_{10}$; ROS: reactive oxygen species. Scale bar: 20 μm.

with the F group. Immunofluorescent images indicated that the nuclear Nrf2 was decreased in AB and AQ groups (Fig. 3D).

The temporal profile dissection of nuclear p-Nrf2 by Western blotting (Suppl. 2A) indicated that the expressions of p-Nrf2 was increased as early as 6 hrs after A53T mutant transfection.

### *tBHQ reversed the A53T-suppressed mitochondrial oxygen consumption rate in N2a cells*

Oxygen consumption rate is a fundamental index of mitochondrial aerobic respiration. The oxygen consumption rate (OCR) measured by the XF24 Extracellular Flux Analyzer (Seahorse) was used to evaluate the maximal respiratory capacity, basal respiratory capacity, and ATP production capacity. Maximal respiratory capacity represented as an indicator of energetic reserve capacity to meet a sudden demand of energy, particularly in high-energy requiring tissues. In this study, we found that the maximal respiratory capacity was significantly suppressed in A53T transfected N2a cells and was rescued by tBHQ (Fig. 4A). Basal respiratory capacity measurement reflects the ROS formation from both coupled and uncoupled oxygen consumption, while ATP production capacity represents the capacity of ATP production by aerobic respiration [38]. The results indicated that there was no significant difference in both basal respiratory capacity (Fig. 4B) and ATP production capacity (Fig. 4C) between F, A, AB or AQ groups. These evidences suggested that SNCA-induced

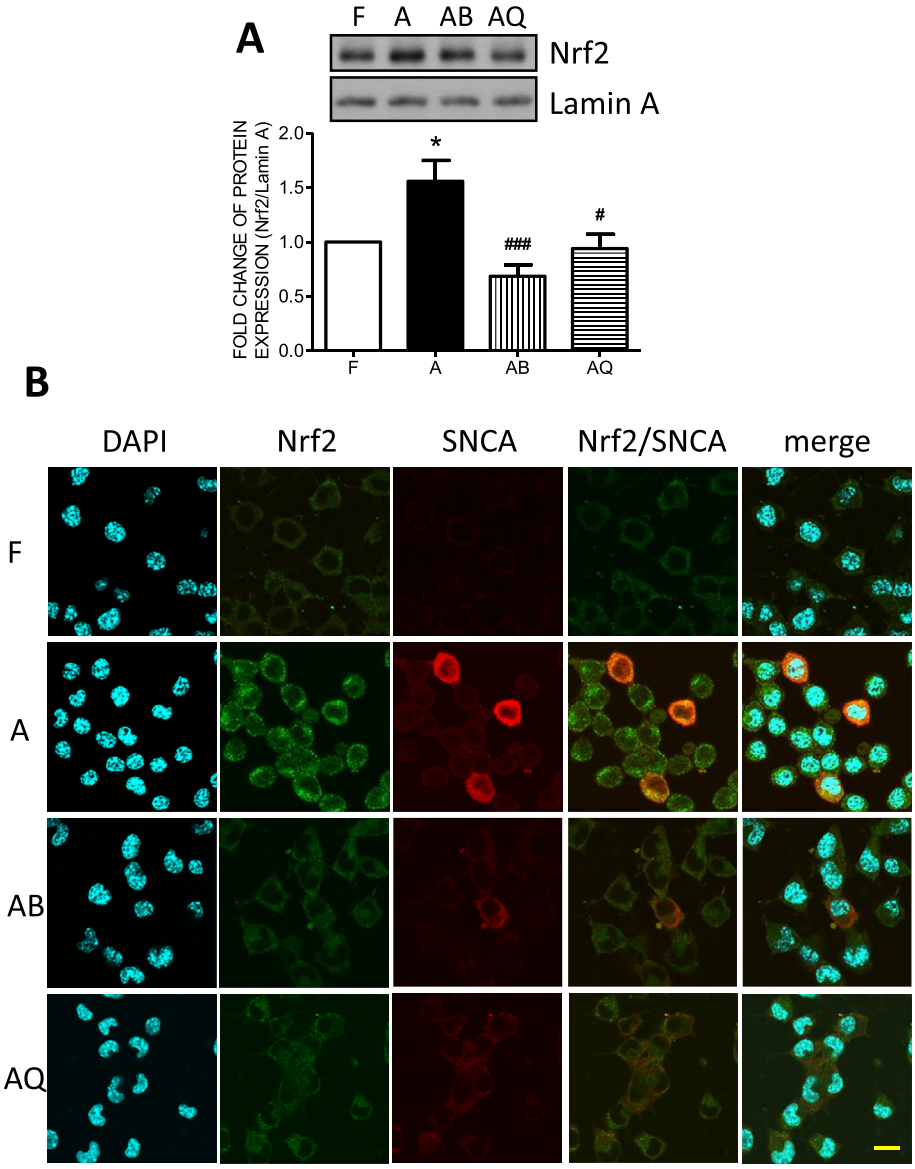


Fig. 3 **tBHQ decreased the nuclear expressions of nuclear Nrf2 and phospho(p)-Nrf2 in A53T mutant transfected N2a cells.** Representative gels and densitometric analyses of nuclear Nrf2 (A) and nuclear p-Nrf2 (C) detected at 48 hrs. Lamin A as loading control. And immunofluorescent of Nrf2 (B, green), p-Nrf2 (D, green), SNCA (red) and DAPI (blue) staining at 48 hrs of F, A, AB and AQ groups. Values are mean ± SEM, n = 6 in each experimental group. $^{\#}p < 0.01$ versus A group in the Post hoc Tukey's multiple ranges tests. Abbreviations used: A: A53T mutant transfected N2a cells; F: N2a cell transfected with FUGW; B: tBHQ; Q: coenzyme $Q_{10}$. Scale bar: 20 μm.

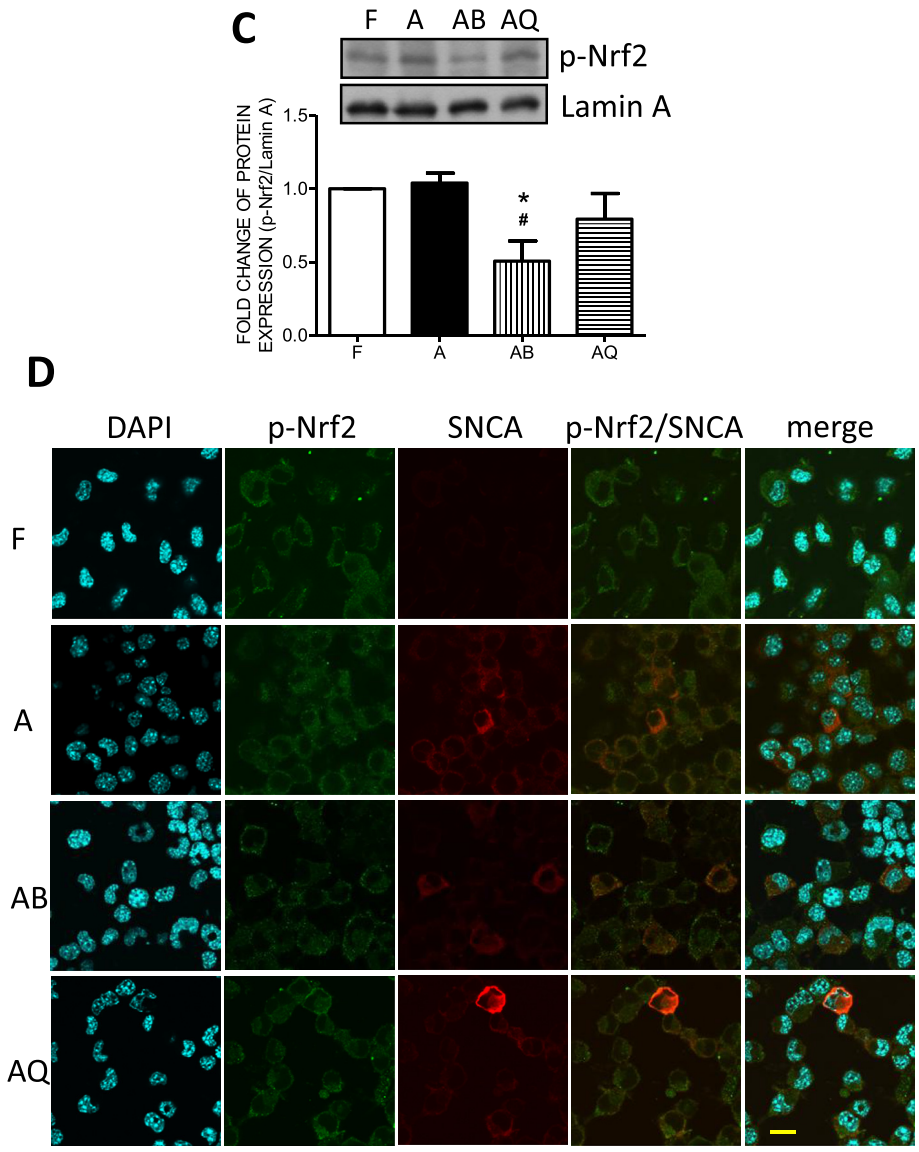


Fig. 3 (*continued*).

oxidative stress mediated the loss of mitochondrial energetic reserve capacity, leading to the failure of high energy demanded. Coenzyme $Q_{10}$ (AQ) is the electron carrier and a well-accepted antioxidant of mitochondria. Adding $Q_{10}$ into A53T cell did not show significant beneficial effect on protecting maximal respiratory capacity from SNCA impairment (Fig. 4). These data imply that the SNCA-induced oxidative stress is upstream to the impairment of mitochondrial oxygen consumption and electron transport reaction.

### *tBHQ reversed the A53T-suppressed mitochondrial respiratory enzyme activity and electron transportation in N2a cells*

Deficiency of respiratory capacity may be a result of dysfunction in the electron transport chain reaction. The electron transport chain reaction is the core of mitochondrial energy production to maintain the neuronal activity. The accumulation of SNCA impairs the function of Mt cpx1 [39]. To delineate whether the electron transport chain reaction was impaired, the enzyme activities of electron transport chain were assayed. Our data indicated that the electron transport activity from Mt cpx1 to 3, known as NCCR activity, in A53T group, was significantly suppressed when compared with FUGW group (Fig. 5A). On the other hand, the electron transport activity from Mt cpx2 to 3, known as SCCR activity, showed no significantly difference between each group (Fig. 5B). These results indicated that the major deficiency occurred at the activity of electron transportation from Mt cpx1 to 3. Furthermore, the enzyme activity of Mt cpx1 was assayed and showed that the activity of Mt cpx1 in A53T N2a cell was significantly decreased in comparison with FUGW cell (Fig. 5C). Incubation with tBHQ effectively reversed the decreased NCCR. On the other hand, application with Coenzyme $Q_{10}$, an electron carrier reacts between Mt cpx1 to 3, showed no effect on reversing the decrease of Mt cpx1-associated activity (Fig. 5).

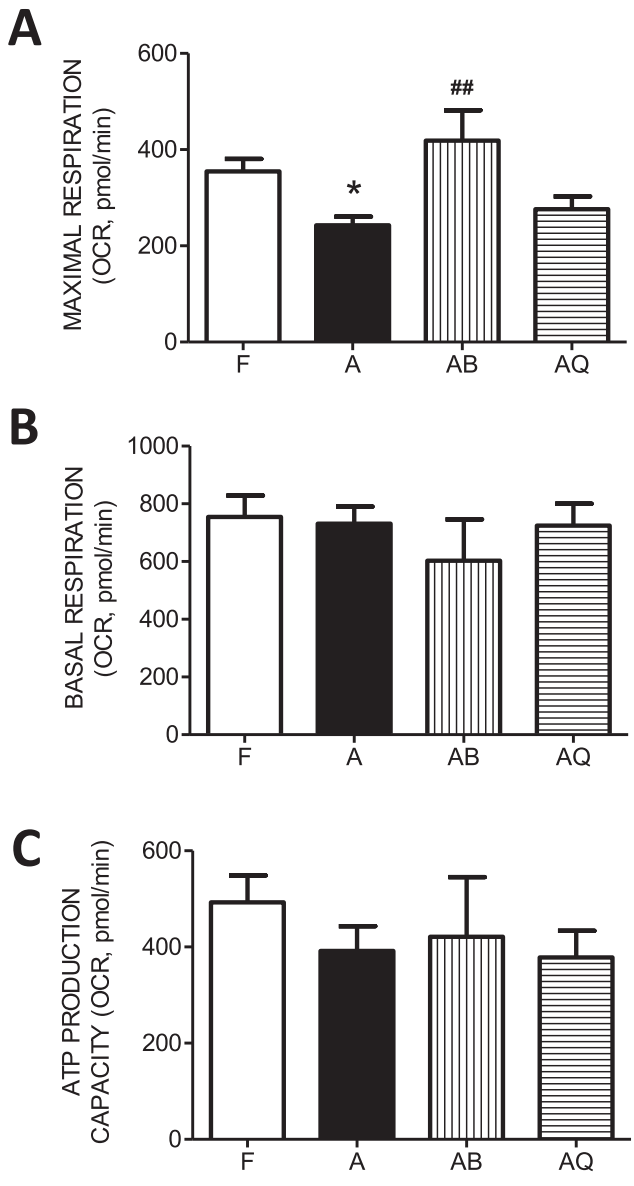


Fig. 4 **The suppression of mitochondrial oxygen consumption rate in A53T mutant transfected N2a cells was reversed by tBHQ.** The maximal respiration capacity (A), the basal respiration capacity (B), and the ATP production capacity (C) detected at 48 h of F, A, AB and AQ groups. Values are mean ± SEM, n = 5 in each experimental group. $^{*}p < 0.05$ versus F group and $^{\#\#}p < 0.01$ versus A group in the Post hoc Tukey's multiple ranges tests. Abbreviations used: A: A53T mutant transfected N2a cells; F: N2a cell transfected with FUGW; B: tBHQ; Q: coenzyme $Q_{10}$.

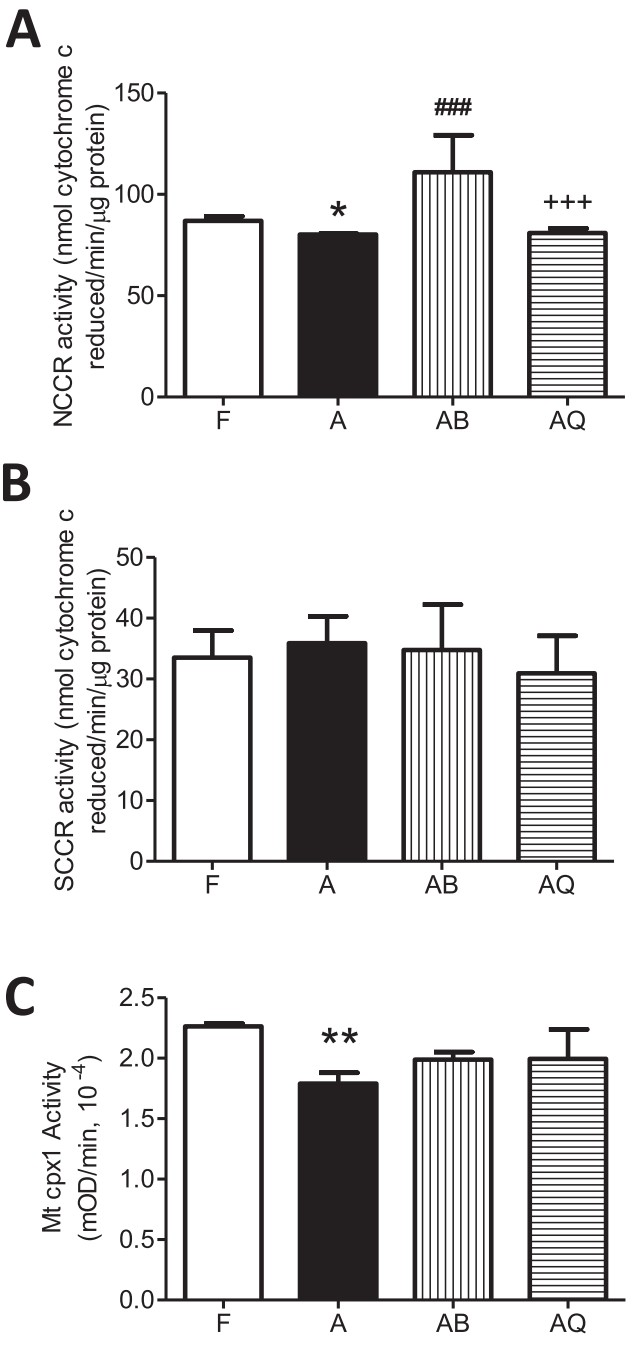


Fig. 5 **The decrease of mitochondrial respiratory activities in A53T mutant transfected N2a cells was reversed by tBHQ.** The activity of NADPH cytochrome C reductase (NCCR) (A), the activity of succinate cytochrome C reductase (SCCR) (B), and the activity of mitochondrial respiratory complex 1 (C) measured at 48 h of F, A, AB and AQ groups. Values are mean ± SEM, n = 5 in each experimental group. $^{*}p < 0.05$, $^{**}p < 0.01$ versus F group and $^{\#\#\#}p < 0.001$ versus A group and $^{+++}P < 0.001$ versus AB group in the Post hoc Tukey's multiple ranges tests. Abbreviations used: A: A53T mutant transfected N2a cells; F: N2a cell transfected with FUGW; B: tBHQ; Q: coenzyme $Q_{10}$.

### *tBHQ reversed the A53T-induced mitochondrial biogenesis impairment in N2a cells*

Mitochondrial biogenesis generates new healthy mitochondria to replace the impaired ones. Dampened mitochondrial biogenesis results in profound suppression of mitochondrial

respiration. The mtDNA copy number and the expression of TFAM are well-accepted indexes of mitochondrial biogenesis. The QPCR results indicated that A53T transfection decreased the mtDNA copy number when compared with FUGW cells and was significantly reversed by tBHQ treatment (Fig. 6A). On the contrary, the expression of TFAM in A53T N2a cells was significantly enhanced, while both tBHQ and coenzyme $Q_{10}$ only partially reversed this effect (Fig. 6B). These results implied that the ability to rebalance the mtDNA decrement was compromised. Coenzyme $Q_{10}$ treatment showed no significant effect on the SNCA-associated mitochondrial biogenesis deficit (Fig. 6).

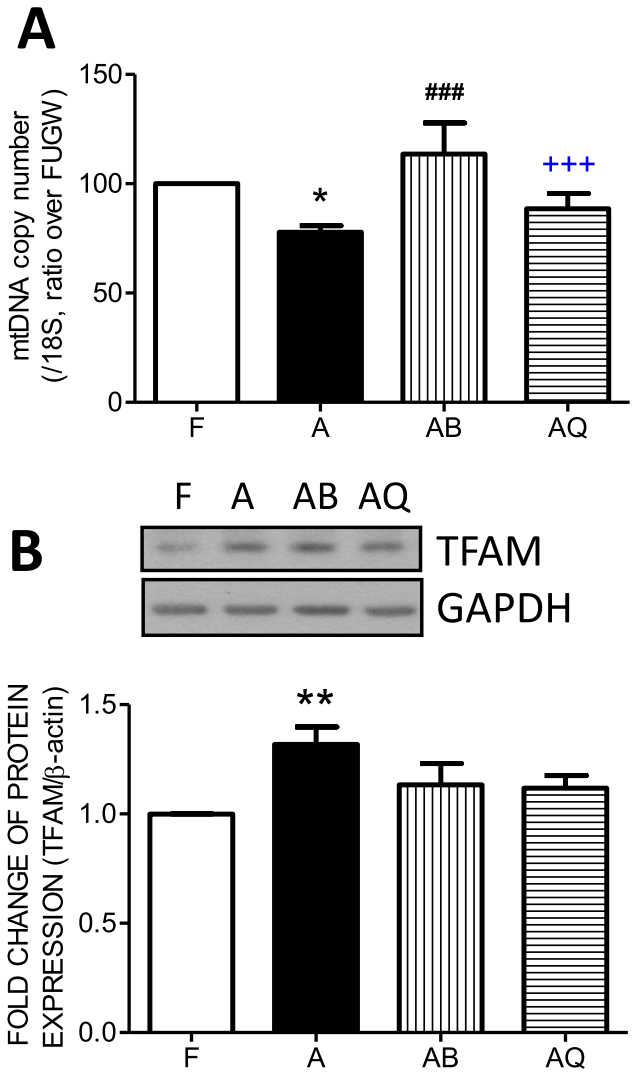


Fig. 6 **The decrease of mitochondrial biogenesis in A53T mutant transfected N2a cells was reversed by tBHQ.** The mitochondrial DNA (mtDNA) copy number (A) detected at 48 h by QPCR. And the representative gel and densitometric analyses of mitochondrial transcription factor A (TFAM) (B) measured at 48 h of F, A, AB and AQ groups. GAPDH as loading control. Values are mean ± SEM, n = 5 in each experimental group. $^{*}p < 0.05$, $^{**}p < 0.01$ versus F group and $^{\#\#\#}p < 0.001$ versus A group and $^{+++}p < 0.001$ versus AB group in the Post hoc Tukey's multiple ranges tests. Abbreviations used: A: A53T mutant transfected N2a cells; F: N2a cell transfected with FUGW; B: tBHQ; Q: coenzyme $Q_{10}$.

PGC-1α is the upstream transcription factor of TFAM. Our data from Western blotting indicated that the expression of nuclear PGC-1α was significantly increased while both tBHQ and coenzyme $Q_{10}$ only partially reversed the increment (Fig. 7A). The immunofluorescent images further indicated that less accumulation of the nuclear PGC-1α in AB and AQ groups when compared with A group (Fig. 7B).

The temporal profile dissection of nuclear PGC-1α and cytosolic TFAM by Western blotting (Suppl. 2B and C) indicated that the expressions of these molecules were increased as early as 6 hrs after A53T mutant transfection.

## Discussion

Our study demonstrated that neurons with SNCA-overexpression decreased maximal respiratory capacity, impaired Mt cpx1 activity, suppressed NCCR activity of ETC reaction, enhanced the mtROS accumulation, and decreased the copy number of mtDNA by using the dopaminergic neural cells transfected with human A53T mutant SNCA. Although nuclear Nrf2 and PGC-1α were increased at earlier stage, trying to enhance the level of TFAM and rescue the mitochondrial damages, their expression was decreased by time and finally resulted in the permanent mitochondrial damage. tBHQ, a common antioxidant and Nrf2 activator, effectively ceased the SNCA-induced impairments. This finding suggested that the SNCA accumulation-induced mtROS mediated the Nrf2/PGC-1α signaling impairment and sequel mitochondrial damages.

Under physiological condition, SNCA localizes in presynaptic nerve terminals and plays important roles in neurotransmission and synaptic maintenance [40,41]. It has been documented that overexpression [42,43] or mutation [9] of *SNCA* gene link to autosomal dominant PD. A53T mutant SNCA results in an overexpression of SNCA and an early-onset of PD [9]. Although a large body of reports from both human and animal studies indicated the co-existence of mitochondrial dysfunction and SNCA overexpression, however, the causal relationship between SNCA and mitochondria is still elusive. These controversies may because while observing at later-stage of PD-like condition, multiple pathogenic factors have been lumped together and may confound the interpretation. To avoid the later-stage observation, we generated the A53T mutant N2a cell line to simulate the earlier-stage of PD with SNCA overexpression but without overt cell death. Through this cell model, the interplay of SNCA and mitochondrial function can be delineated more straightforwardly.

Oxidative stress is a critical factor in the degeneration of dopaminergic neurons in PD. However, the interplay of SNCA and oxidative stress is under debate. Some experiments indicated that increased oxidative stress contributing to SNCA aggregation [44–46]. On the other hand, growing evidences suggested that SNCA overexpression promotes the increase of ROS production [26,47,48]. In our *in vitro* model, we found that SNCA overexpression resulted in ROS accumulation in mitochondria before the initiation of cell death. Both tBHQ and

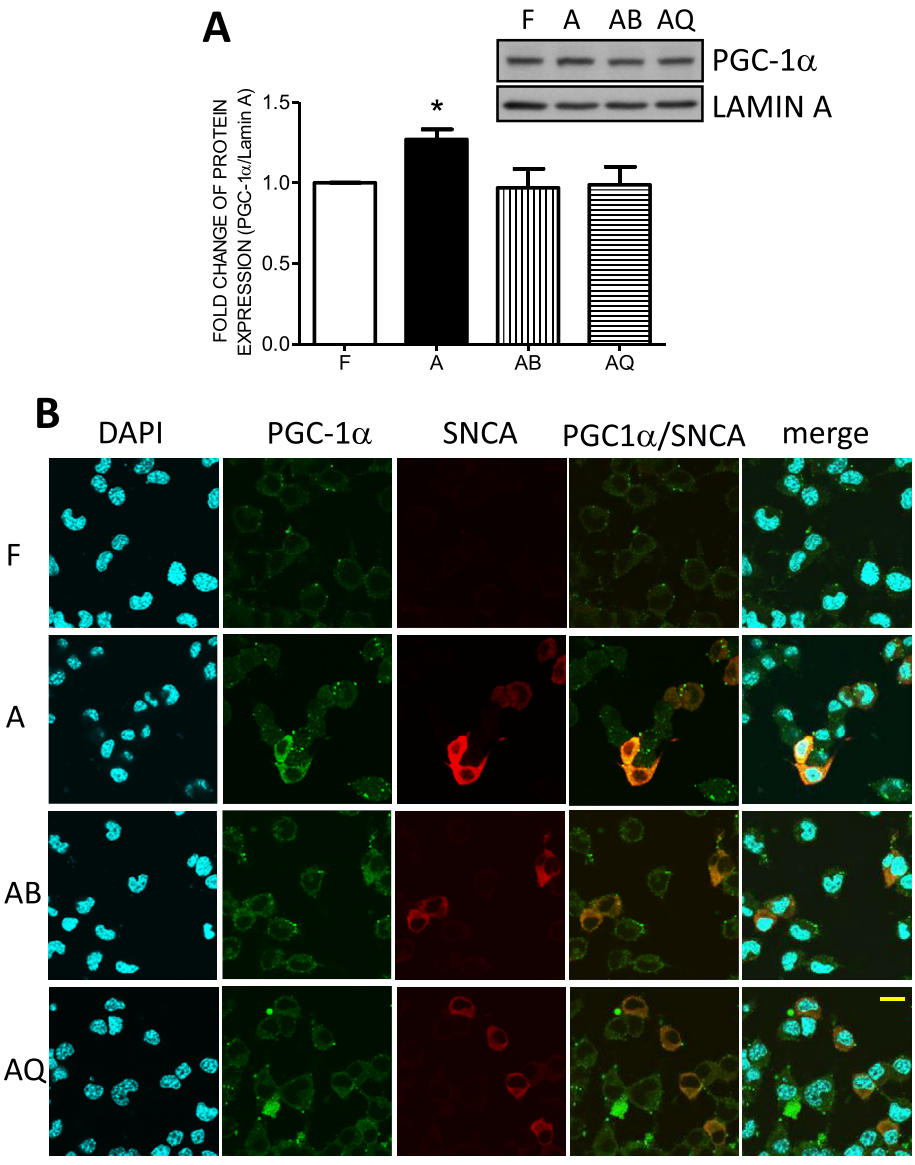


Fig. 7 **The increase of nuclear PGC-1α in A53T mutant transfection N2a cells was reduced by tBHQ.** (A) The representative gel and densitometric analyses of peroxisome proliferator-activated receptor γ coactivator 1-α (PGC-1α). Lamin A as loading control. (B) Immunofluorescent of PGC-1α (green), SNCA (red) and DAPI (blue) staining at 48 h of F, A, AB and AQ groups. Values are mean ± SEM, n = 5 in each experimental group. $^{*}p < 0.05$ versus FUGW in the post hoc Tukey's multiple ranges tests. Abbreviations used: A: A53T mutant transfected N2a cells; F: N2a cell transfected with FUGW; B: tBHQ; Q: coenzyme $Q_{10}$. Scale bar: 20 μm.

coenzyme $Q_{10}$ are well known antioxidants for ROS scavenge. Intriguingly, treatment with tBHQ effectively abolished the mtROS accumulation, while coenzyme $Q_{10}$ treatment showed no effect on diminishing mtROS. tBHQ is a well-known Nrf2 activator and coenzyme $Q_{10}$ is the electron carrier of ETC. These observations implied that the SNCA-induced cytosolic oxidative stress could be the upstream signaling of mtROS accumulation. Numerous mechanisms have been proposed to induce ROS generation after SNCA accumulation, including mitochondrial dysfunction, neuroinflammation, dopamine, iron, calcium and aging. For the limitation of the study design, the source for SNCA-induced ROS at earlier stage is currently unidentified.

As an inducible transcription factor, Nrf2 encodes multiple antioxidants. It is known that Nrf2 is negatively regulated by the Kelch-like ECH-associated protein 1 (Keap1)-Cullin3 (Cul3)/Rbx1 under physiological condition [49,50] and oxidants release Nrf2 from Keap1 [51]. Our studies indicated that the expression and nuclear translocation of Nrf2 were increased after SNCA overexpression before the cell death process being programmed. The result also hinted the increment of oxidative stress in the SNCA-overexpressed neurons. Western blotting analyses further indicated that tBHQ treatment effectively reduced nuclear Nrf2 accumulation. In the immunofluorescent images, both nuclear and cytosolic Nrf2 accumulation induced by SNCA

overexpression vanished after adding antioxidants. These data showed that tBHQ could ameliorate SNCA-induced oxidative stress. Further, tBHQ treatment effectively reduced the p-Nrf2 in nuclei suggested the entrance of p-Nrf2 was for oxidant defense. The inconsistence of the nuclear p-Nrf2 and nuclear Nrf2 accumulation could be the result of different specificity of Nrf2 and p-Nrf2 antibodies being used in our study.

By temporal profile dissection, we found that the expression of nuclear p-Nrf2 was upregulated to the plateau levels after treating tBHQ or coenzyme $Q_{10}$ for 6 hrs in the A53T transfected cells. These data suggested that in response to the oxidative stress induced by SNCA, Nrf2 was activated and translocated to nucleus for oxidant defense. Moreover, the fluctuation level of nuclear p-Nrf2 expression 48 hrs after transfection further outline the profile of oxidative status triggered by SNCA overexpression. Similar patterns were detected in nuclear PGC-1α and cytosolic TFAM expressions. Previous studies indicated that Nrf2 is involved in the regulation of mitochondrial homeostasis and oxidant defense [52]. These results suggested the upregulation of nuclear Nrf2 and PGC-1α were in fact response to the SNCA-induced stress, aiming to defend the oxidative stress and to maintain mitochondrial quality. From the declined pattern of nuclear Nrf2 and PGC-1α, prolonged SNCA accumulation may eventually impair the Nrf2/PGC-1α protection mechanism and lead to permanent mitochondrial damage. Activation of Nrf2 by tBHQ promotes mitochondrial biogenesis in neurons [35].

Mitochondrial dysfunction contributes to the pathogenesis of PD has been demonstrated since 1979 [53]. However, the trigger to initiate the process of mitochondrial dysfunction is still under investigation. Mitochondria are an indispensable resource of cell energy. If the energy demand is unmet, the net result will be cell senescence and death in the affected tissue. The term, maximal respiratory capacity, is used to describe the total amount of energy that can be produced by oxidative phosphorylation in case of a sudden increase in energy demand. Previous studies in cybrid cell line suggested that SNCA aggregation suppresses basal respiratory capacity, ATP production capacity, and maximal respiratory capacity, finally leading to cell death [20]. At the stage without profound cell death, we found that SNCA accumulation significantly suppressed the maximal respiratory capacity of N2a cells. The low capacity of energy production to meet a sudden high-energy demand in neurons may be the trigger for sequel pathogenesis at earlier stage of SNCA accumulation. tBHQ treatment effectively reversed the suppression of the maximal respiratory capacity further verified the role of SNCA-induced oxidative stress in the impaired mitochondrial respiratory capacity at earlier stage.

Oxidative phosphorylation is the core of energy synthesis driven by electron transport chain. The electron transportation from Mt cpx1 or Mt cpx2 to Mt cpx3 by electron carrier via coenzyme $Q_{10}$ is the common pathway to generate the driving force of energy production. Mt cpx1 dysfunction has been well documented in synucleinopathy [39,54,55]. According to the enzyme activity assays, our data indicated that the activities of NCCR of SNCA-overexpressed neurons were significantly suppressed while the SCCR showed no significantly changes between groups. In consistence with previous studies [39,54,55], the enzyme activity of Mt cpx1 in the SNCA-overexpressed neurons was significantly decreased. These results suggested that the deficiency of mitochondrial oxidative phosphorylation in the SNCA-overexpressed neurons was a specific result of Mt cpx1 impairment, followed by suppression of electron transportation from Mt cpx1 to Mt cpx3. tBHQ effectively preventing the impairment of Mt cpx1 further supported the potential mechanism that SNCA-induced oxidative stress mainly damages the Mt cpx1 function at earlier stage. These evidences confirmed that Mt cpx1 is the main target of SNCA-associated mitochondrial impairment. Reversing oxidative stress was able to rebalance the Mt cpx1-associated decrement of NCCR activity. Coenzyme $Q_{10}$ treatment showed no significant protection effect on NCCR activity. Together with the oxygen consumption data, this finding further indicated that the SNCA-induced oxidative stress is upstream to the impairment of mitochondrial oxygen consumption and ETC. Impairments of Mt cpx1 function and ETC are major sources of mtROS [56]. For ROS-induced mtROS generation has been proposed in other studies [25], our present study further indicated that SNCA-induced oxidative stress impairs mitochondrial energy metabolism which may lead to the increase of mtROS generation. It is reasonable that coenzyme $Q_{10}$, as the electron carrier, is not able to reverse the ETC activity decrement impaired by upstream insults.

Mitochondrial biogenesis responds for the mitochondrial renewal to replace the impaired mitochondria. Thus, the impairment of mitochondrial biogenesis results in decline of mitochondrial quality control. The reduction of mitochondrial DNA copy number has been demonstrated in the brain of PD [57]. In consistent with these later-stage studies, our study further indicated that the mtDNA copy numbers was mild and significantly suppressed in the SNCA-overexpressed N2a cells. PGC-1α is the key regulator of mitochondrial biogenesis and regulates the expression of TFAM to increase mtDNA transcription and translation. On the contrary, the expressions of cytosolic TFAM and nuclear PGC-1α showed significantly increased in SNCA-overexpressed neurons. These increments may be a compensatory effect to maintain mitochondrial function under the early stage of pathogenesis. The immunofluorescent images further indicated that the nuclear PGC-1α was mild accumulated in SNCA-overexpressed-neurons while the nuclear signal was vanished by antioxidant treatments. These evidences further suggested that the accumulation of PGC-1α in nuclei resulted from the enhanced oxidative stress. The temporal profile of nuclear PGC-1α expressions showed a synchronic with p-Nrf2 and intermittent increase at 6 and 24 h after A53T transfection. These evidences suggested an early activation of Nrf2 which may relate to the enhancement of nuclear PGC-1α and cytosolic TFAM to rebalance the mitochondrial function at the early stage of SNCA accumulation.

By using a cell model to mimic genetic insults of dopaminergic neuron in PD, we demonstrated that the oxidative stress induced by SNCA-overexpression results in limited maximal respiratory capacity, suppression of Mt cpx1 enzyme activity, reduction of NCCR activity, and decrement of mtDNA

copy number at earlier-stage of PD-simulating cell environment. Concurrently, Nrf2 activation was enhanced at this stage, trying to overcome these adverse effects of oxidative stress and rescue the function of mitochondria.

## Conflicts of interest

The authors declare no conflicts of interest.

## Acknowledgement

This study was supported by grants from the Chang Gung Medical Foundation (CMRPG8D0971, CMRPG8E0701 and CPRPG8F1661 to MHF).

## Appendix A. Supplementary data

Supplementary data related to this article can be found at https://doi.org/10.1016/j.bj.2018.02.005

## REFERENCES

[1] Forno LS. Neuropathology of Parkinson's disease. J Neuropathol Exp Neurol 1996;55:259–72.
[2] McCann H, Stevens CH, Cartwright H, Halliday GM. alpha-Synucleinopathy phenotypes. Park Relat Disord 2014;20(Suppl 1):S62–7.
[3] Fink AL. The aggregation and fibrillation of alpha-synuclein. Acc Chem Res 2006;39:628–34.
[4] Anderson JP, Walker DE, Goldstein JM, de Laat R, Banducci K, Caccavello RJ, et al. Phosphorylation of Ser-129 is the dominant pathological modification of alpha-synuclein in familial and sporadic Lewy body disease. J Biol Chem 2006;281:29739–52.
[5] Fujiwara H, Hasegawa M, Dohmae N, Kawashima A, Masliah E, Goldberg MS, et al. alpha-Synuclein is phosphorylated in synucleinopathy lesions. Nat Cell Biol 2002;4:160–4.
[6] Neumann M, Kahle PJ, Giasson BI, Ozmen L, Borroni E, Spooren W, et al. Misfolded proteinase K-resistant hyperphosphorylated alpha-synuclein in aged transgenic mice with locomotor deterioration and in human alpha-synucleinopathies. J Clin Invest 2002;110:1429–39.
[7] Schell H, Hasegawa T, Neumann M, Kahle PJ. Nuclear and neuritic distribution of serine-129 phosphorylated alpha-synuclein in transgenic mice. Neuroscience 2009;160:796–804.
[8] Kruger R, Kuhn W, Muller T, Woitalla D, Graeber M, Kosel S, et al. Ala30Pro mutation in the gene encoding alpha-synuclein in Parkinson's disease. Nat Genet 1998;18:106–8.
[9] Polymeropoulos MH, Lavedan C, Leroy E, Ide SE, Dehejia A, Dutra A, et al. Mutation in the alpha-synuclein gene identified in families with Parkinson's disease. Science 1997;276:2045–7.
[10] Zarranz JJ, Alegre J, Gomez-Esteban JC, Lezcano E, Ros R, Ampuero I, et al. The new mutation, E46K, of alpha-synuclein causes Parkinson and Lewy body dementia. Ann Neurol 2004;55:164–73.
[11] Narhi L, Wood SJ, Steavenson S, Jiang Y, Wu GM, Anafi D, et al. Both familial Parkinson's disease mutations accelerate alpha-synuclein aggregation. J Biol Chem 1999;274:9843–6.
[12] Blesa J, Phani S, Jackson-Lewis V, Przedborski S. Classic and new animal models of Parkinson's disease. J Biomed Biotechnol 2012;2012:845618.
[13] Giasson BI, Duda JE, Quinn SM, Zhang B, Trojanowski JQ, Lee VM. Neuronal alpha-synucleinopathy with severe movement disorder in mice expressing A53T human alpha-synuclein. Neuron 2002;34:521–33.
[14] Kahle PJ, Neumann M, Ozmen L, Muller V, Jacobsen H, Schindzielorz A, et al. Subcellular localization of wild-type and Parkinson's disease-associated mutant alpha -synuclein in human and transgenic mouse brain. J Neurosci 2000;20:6365–73.
[15] Pandey N, Schmidt RE, Galvin JE. The alpha-synuclein mutation E46K promotes aggregation in cultured cells. Exp Neurol 2006;197:515–20.
[16] Choi W, Zibaee S, Jakes R, Serpell LC, Davletov B, Crowther RA, et al. Mutation E46K increases phospholipid binding and assembly into filaments of human alpha-synuclein. FEBS lett 2004;576:363–8.
[17] Mbefo MK, Fares MB, Paleologou K, Oueslati A, Yin G, Tenreiro S, et al. Parkinson disease mutant E46K enhances alpha-synuclein phosphorylation in mammalian cell lines, in yeast, and in vivo. J Biol Chem 2015;290:9412–27.
[18] Sato H, Kato T, Arawaka S. The role of Ser129 phosphorylation of alpha-synuclein in neurodegeneration of Parkinson's disease: a review of in vivo models. Rev Neurosci 2013;24:115–23.
[19] Thomas B, Beal MF. Parkinson's disease. Hum Mol Genet 2007;16:R183–94.
[20] Reeve AK, Ludtmann MH, Angelova PR, Simcox EM, Horrocks MH, Klenerman D, et al. Aggregated alpha-synuclein and complex I deficiency: exploration of their relationship in differentiated neurons. Cell Death Dis 2015;6, e1820.
[21] Kamp F, Exner N, Lutz AK, Wender N, Hegermann J, Brunner B, et al. Inhibition of mitochondrial fusion by alpha-synuclein is rescued by PINK1, Parkin and DJ-1. EMBO J 2010;29:3571–89.
[22] Nakamura K, Nemani VM, Azarbal F, Skibinski G, Levy JM, Egami K, et al. Direct membrane association drives mitochondrial fission by the Parkinson disease-associated protein alpha-synuclein. J Biol Chem 2011;286:20710–26.
[23] Devi L, Raghavendran V, Prabhu BM, Avadhani NG, Anandatheerthavarada HK. Mitochondrial import and accumulation of alpha-synuclein impair complex I in human dopaminergic neuronal cultures and Parkinson disease brain. J Biol Chem 2008;283:9089–100.
[24] Keeney PM, Xie J, Capaldi RA, Bennett Jr JP. Parkinson's disease brain mitochondrial complex I has oxidatively damaged subunits and is functionally impaired and misassembled. J Neurosci 2006;26:5256–64.
[25] Zorov DB, Juhaszova M, Sollott SJ. Mitochondrial reactive oxygen species (ROS) and ROS-induced ROS release. Physiol Rev 2014;94:909–50.
[26] Junn E, Mouradian MM. Human alpha-synuclein over-expression increases intracellular reactive oxygen species levels and susceptibility to dopamine. Neurosci Lett 2002;320:146–50.
[27] Ishii T, Itoh K, Takahashi S, Sato H, Yanagawa T, Katoh Y, et al. Transcription factor Nrf2 coordinately regulates a group of oxidative stress-inducible genes in macrophages. J Biol Chem 2000;275:16023–9.
[28] Lastres-Becker I, Ulusoy A, Innamorato NG, Sahin G, Rabano A, Kirik D, et al. alpha-Synuclein expression and Nrf2

deficiency cooperate to aggravate protein aggregation, neuronal death and inflammation in early-stage Parkinson's disease. Hum Mol Genet 2012;21:3173–92.
[29] Barone MC, Sykiotis GP, Bohmann D. Genetic activation of Nrf2 signaling is sufficient to ameliorate neurodegenerative phenotypes in a Drosophila model of Parkinson's disease. Dis Model Mech 2011;4:701–7.
[30] Jornayvaz FR, Shulman GI. Regulation of mitochondrial biogenesis. Essays Biochem 2010;47:69–84.
[31] Martin LJ, Pan Y, Price AC, Sterling W, Copeland NG, Jenkins NA, et al. Parkinson's disease alpha-synuclein transgenic mice develop neuronal mitochondrial degeneration and cell death. J Neurosci 2006;26:41–50.
[32] Michel PP, Hirsch EC, Hunot S. Understanding dopaminergic cell death pathways in Parkinson disease. Neuron 2016;90:675–91.
[33] Wu KLH, Wu CW, Tain YL, Huang LT, Chao YM, Hung CY, et al. Environmental stimulation rescues maternal high fructose intake-impaired learning and memory in female offspring: its correlation with redistribution of histone deacetylase 4. Neurobiol Learn Mem 2016;130:105–17.
[34] Wu KLH, Hsu C, Chan JYH. Impairment of the mitochondrial respiratory enzyme activity triggers sequential activation of apoptosis-inducing factor-dependent and caspase-dependent signaling pathways to induce apoptosis after spinal cord injury. J Neurochem 2007;101:1552–66.
[35] Wu KLH, Wu CW, Chao YM, Hung CY, Chan JY. Impaired Nrf2 regulation of mitochondrial biogenesis in rostral ventrolateral medulla on hypertension induced by systemic inflammation. Free Radic Biol Med 2016;97:58–74.
[36] Varcin M, Bentea E, Michotte Y, Sarre S. Oxidative stress in genetic mouse models of Parkinson's disease. Oxid Med Cell Longev 2012;2012:624925.
[37] Skibinski G, Hwang V, Ando DM, Daub A, Lee AK, Ravisankar A, et al. Nrf2 mitigates LRRK2- and alpha-synuclein-induced neurodegeneration by modulating proteostasis. Proc Natl Acad Sci U S A 2017;114:1165–70.
[38] Hartman ML, Shirihai OS, Holbrook M, Xu G, Kocherla M, Shah A, et al. Relation of mitochondrial oxygen consumption in peripheral blood mononuclear cells to vascular function in type 2 diabetes mellitus. Vasc Med 2014;19:67–74.
[39] Langston JW, Ballard P, Tetrud JW, Irwin I. Chronic Parkinsonism in humans due to a product of meperidine-analog synthesis. Science 1983;219:979–80.
[40] Bendor JT, Logan TP, Edwards RH. The function of alpha-synuclein. Neuron 2013;79:1044–66.
[41] Maroteaux L, Campanelli JT, Scheller RH. Synuclein: a neuron-specific protein localized to the nucleus and presynaptic nerve terminal. J Neurosci 1988;8:2804–15.
[42] Chartier-Harlin MC, Kachergus J, Roumier C, Mouroux V, Douay X, Lincoln S, et al. Alpha-synuclein locus duplication as a cause of familial Parkinson's disease. Lancet 2004;364:1167–9.
[43] Singleton AB, Farrer M, Johnson J, Singleton A, Hague S, Kachergus J, et al. alpha-Synuclein locus triplication causes Parkinson's disease. Science 2003;302:841.
[44] Hashimoto M, Hsu LJ, Xia Y, Takeda A, Sisk A, Sundsmo M, et al. Oxidative stress induces amyloid-like aggregate formation of NACP/alpha-synuclein in vitro. Neuroreport 1999;10:717–21.
[45] Paxinou E, Chen Q, Weisse M, Giasson BI, Norris EH, Rueter SM, et al. Induction of alpha-synuclein aggregation by intracellular nitrative insult. J Neurosci 2001;21:8053–61.
[46] Esteves AR, Arduino DM, Swerdlow RH, Oliveira CR, Cardoso SM. Oxidative stress involvement in alpha-synuclein oligomerization in Parkinson's disease cybrids. Antioxid Redox Signal 2009;11:439–48.
[47] Deas E, Cremades N, Angelova PR, Ludtmann MH, Yao Z, Chen S, et al. Alpha-synuclein oligomers interact with metal ions to induce oxidative stress and neuronal death in Parkinson's disease. Antioxid Redox Signal 2016;24:376–91.
[48] Winklhofer KF, Haass C. Mitochondrial dysfunction in Parkinson's disease. Biochim Biophys Acta 2010;1802:29–44.
[49] Itoh K, Wakabayashi N, Katoh Y, Ishii T, Igarashi K, Engel JD, et al. Keap1 represses nuclear activation of antioxidant responsive elements by Nrf2 through binding to the amino-terminal Neh2 domain. Genes Dev 1999;13:76–86.
[50] Zhang DD, Lo SC, Cross JV, Templeton DJ, Hannink M. Keap1 is a redox-regulated substrate adaptor protein for a Cul3-dependent ubiquitin ligase complex. Mol Cell Biol 2004;24:10941–53.
[51] Zhang DD, Hannink M. Distinct cysteine residues in Keap1 are required for Keap1-dependent ubiquitination of Nrf2 and for stabilization of Nrf2 by chemopreventive agents and oxidative stress. Mol Cell Biol 2003;23:8137–51.
[52] Dinkova-Kostova AT, Abramov AY. The emerging role of Nrf2 in mitochondrial function. Free Radic Biol Med 2015;88:179–88.
[53] Davis GC, Williams AC, Markey SP, Ebert MH, Caine ED, Reichert CM, et al. Chronic Parkinsonism secondary to intravenous injection of meperidine analogues. Psychiatr Res 1979;1:249–54.
[54] Betarbet R, Sherer TB, MacKenzie G, Garcia-Osuna M, Panov AV, Greenamyre JT. Chronic systemic pesticide exposure reproduces features of Parkinson's disease. Nat Neurosci 2000;3:1301–6.
[55] Keane PC, Kurzawa M, Blain PG, Morris CM. Mitochondrial dysfunction in Parkinson's disease. Parkinsons Dis 2011;2011:716871.
[56] Hoffman DL, Brookes PS. Oxygen sensitivity of mitochondrial reactive oxygen species generation depends on metabolic conditions. J Biol Chem 2009;284:16236–45.
[57] Pyle A, Anugrha H, Kurzawa-Akanbi M, Yarnall A, Burn D, Hudson G. Reduced mitochondrial DNA copy number is a biomarker of Parkinson's disease. Neurobiol Aging 2016;38:216.e7–e10.